

# Modulation Depth Based on Frequency-shift Characteristic of LiNbO<sub>3</sub> Waveguide Electro-optic Intensity Modulator

Hui-juan ZHOU(周会娟), Zhou MENG(孟 洲), Yi LIAO(廖 毅)

(College of Optoelectronic Science and Engineering, National University of Defense Technology, Changsha 410073, China)

**Abstract** – The modulation depth, defined according to practical modulation results, which changes with the microwave power and its frequency, is significant for systems utilizing the frequency-shift characteristic of the LiNbO<sub>3</sub> waveguide Electro-Optic Intensity Modulator (EOIM). By analyzing the impedance mismatch between the microwave source and the EOIM, the effective voltage applied to the RF port of the EOIM is deprived from the microwave power and its frequency. Associating with analyses of the phase velocity mismatch between the microwave and the optical wave, the theoretical modulation depth has been obtained, which is verified by experimental results. We provide a method to choose the appropriate modulation depth to optimize the desired sideband through proper transmission bias for the system based on the frequency-shift characteristic of the EOIM.

**Key Words:** LiNbO<sub>3</sub> waveguide electro-optic intensity modulator; modulation depth; frequency shift; distributed Brillouin optical fiber sensing

**Manuscript Number:** 1674-8042(2010)02-0125-04

**doi:** 10.3969/j.issn.1674-8042.2010.02.06

## 1 Introduction

For its excellent frequency-shift characteristic, the LiNbO<sub>3</sub> waveguide Electro-Optic Intensity Modulator (EOIM) has been widely applied to distributed Brillouin optical fiber sensing<sup>[1-3]</sup>, high-frequency millimeter-wave generation<sup>[4]</sup>, and Optical Single-Sideband Modulation (OSSB)<sup>[5]</sup>, etc. Based on its better performance in frequency shift than a electro-optic phase modulator, it is not impossible that the EOIM can be used to generate multi-wavelength source as a phase modulator does<sup>[6]</sup>. Especially, considering the 11 GHz frequency shift (at 1.55  $\mu\text{m}$ ) between the Brillouin scattering light and the input light, the EOIM provides an excellent solution to detect the slight Brillouin sensing signal for distributed Brillouin optical fiber sensing systems<sup>[7]</sup>. In our previous work, a comprehensive study was presented on the frequency-shift performance of the EOIM and some significant results were

obtained<sup>[8-10]</sup>. Modulation depth, which is defined according to practical microwave modulation results, mainly affects amplitudes of modulated sidebands. It should be noted that the modulation depth here is different from the definition in optical communication<sup>[11-14]</sup>. They focus on characteristics of the component itself while we care about the applications of the modulator based on its frequency shift characteristic.

We find that the modulation depth increases with the modulated signal power but decreases with the increasing modulated frequency. Although the true modulation depth can be obtained through the ratio of different sidebands' intensities after modulation<sup>[10]</sup>, what's more significant is how to choose the proper microwave power and its frequency aiming at the appropriate modulation depth before experiments. Once the modulator is packaged, its characteristics, such as the impedance, the modulation band, and the driving voltage, etc., are settled. Since the modulation depth has nothing to do with the optical wave transmitting in the modulator, it can be calculated from the modulated signal (microwave power and its frequency) through these intrinsic characteristics. Here we analyze the dependence of the modulation depth on microwave power and its frequency from two aspects and give out the exact estimation through microwave parameters (like S11) of the modulator. Experimental results demonstrate the theoretical analyses well, which provides a method for systems utilizing the EOIM to choose an appropriate modulation depth to obtain the optimal modulated sideband.

## 2 Theory

The EOIM adopts traveling-wave electrodes and Mach-Zehnder interferometer waveguides as shown in Fig. 1. Suppose that the modulated signal applied on the RF port of the EOIM is

$$V = V_m \cos(\omega_m t), \quad (1)$$

\* Received: 2010-02-25

Project supported: This work is supported by Program for New Century Excellent Talents in University (No. NCET-06-0925)

Corresponding author: Zhou MENG(zhoumeng6806@163.com)

where  $V_m$  is the amplitude of the modulated signal and  $\omega_m$  is the modulated angular frequency, in conjunction with the Direct Current (DC) bias voltage  $V_{DC}$  applied to the DC port.

The optical phase difference at the output end of the modulator,  $\Delta\varphi$ , is expressed as

$$\Delta\varphi = \pi \frac{V_{DC}}{2V_\pi} + \pi \frac{V_m}{2V_\pi} \cos(\omega_m t), \quad (2)$$

where  $V_\pi$  is the half-wavelength voltage of the modulator. Modulation depth,  $C$ , is then given by

$$C = \pi \frac{V_m}{2V_\pi}. \quad (3)$$

Thus, the electrical field of the output light at the end of the modulator is described by<sup>[8]</sup>

$$E = E_0 \cos(\omega_0 t) \left\{ \begin{aligned} & [J_0(C) + 2 \sum_{n=1}^{\infty} (-1)^n J_{2n}(C) \cos(2n\omega_m t)] \cos\varphi_{DC} \\ & - [2 \sum_{n=0}^{\infty} (-1)^n J_{2n+1}(C) \cos(2n+1)\omega_m t] \sin\varphi_{DC} \end{aligned} \right\}. \quad (4)$$

where  $E_0$  is the amplitude of the input electrical field of the light,  $\varphi_{DC} = \pi V_{DC}/2V_\pi$  is the phase difference induced by  $V_{DC}$ ,  $\omega_0$  is the optical angular frequency,  $J_n$  is the Bessel function of the  $n^{\text{th}}$ -order. As Eq. (4) shows, for some sideband, its intensity completely depends on the  $C$  value while the input light and the DC bias are fixed. Limited by the tolerable input optical power and the modulated signal (microwave power and frequency) of the EOIM, the modulation depth must be confined to certain range. On the other hand, the modulation depth is not the higher the better according to the trend of the  $n^{\text{th}}$ -order Bessel function versus  $C$ . Thus, it is necessary to predict that the appropriate modulation depth before modulation rather than modifying the true values obtained by the ratio of different-even/odd-order sidebands after modulation is as shown in Eq. (4).

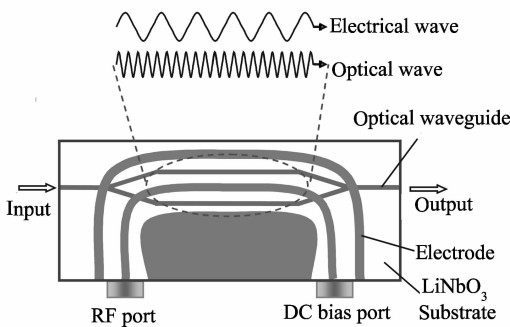


Fig.1 Schematic of a traveling-wave type EOIM

The estimation starts from Eq. (3), which indicates that the modulation depth  $C$  depends on characteristics of the modulator itself ( $V_\pi$ ), and the modulated signal ( $V_m$ ).  $V_\pi$  can be obtained by the static measurement of the modulator. The key problem here is how to get the effective modulation voltage  $V_m$  applied to the EOIM when the modulated power  $P_m$  and frequency  $f_m$  are given. In

Ref. [10], it indicates that two factors determine the modulation efficiency. One is the impedance mismatch between the microwave source and the modulator; the other is the phase velocity mismatch between the optical wave and the microwave. We will develop an exact equation of  $C$  versus  $P_m$  and  $f_m$  in terms of the above two factors in the following.

## 2.1 Impedance mismatch between the microwave source and the modulator

The EOIM is a microwave component connecting to the microwave source through a SMA connector. Usually, the impedance of the microwave source is  $50 \Omega$  while the characteristic impedance of the EOIM changes with the microwave frequency, which results in the power reflection from the modulator to the source. That is to say, the output power of the source can not be completely applied to the modulator. The power reflection coefficient ( $S_{11}$ ) is used to depict the reflection level. Fig.2 shows  $S_{11}$  values of the EOIM we use. Stars in the figure show calculated results obtained from measured characteristic impedances, while the curve shows the corresponding  $S_{11}$  scanned by a vector network analyzer (Agilent E8363B), the two of which are coincident. As  $S_{11}$  is below  $-10$  dB from 1 GHz to 15 GHz (chosen according to the specification of the EOIM), the impedance matching is sufficient with respect to the standard of the modulator in optical communications<sup>[15]</sup>. In other words, however, there is at least 10% microwave power reflected to the source. Therefore, to calculate the effective voltage applied to the modulator, the parameter  $S_{11}$  should be taken into consideration. As the  $S_{11}$  is usually given by dB, the effective voltage at the RF input port of the electrode is then given by

$$V_{m0} = \sqrt{2P_m (1 - 10^{S_{11}/10}) Z_s}, \quad (5)$$

where  $Z_s = 50 \Omega$  is the standard impedance of the microwave source.

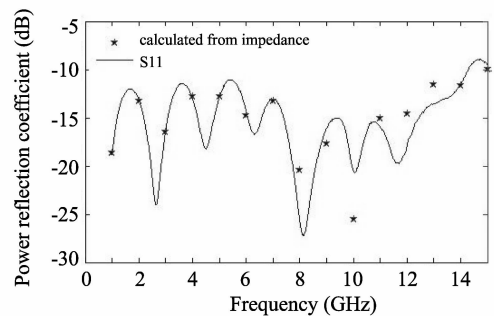


Fig.2 Power reflection coefficient ( $S_{11}$ ) of the EOIM

It should be noted that  $V_{m0}$  is calculated from the microwave power and its frequency is usually given by the microwave source. A new parameter,  $C_0$ , is defined as

$$C_0 = \pi \frac{V_{m0}}{2V_\pi}, \quad (6)$$

$V_{m0}$  and  $C_0$  here are different from  $V_m$  and  $C$ , because  $V_{m0}$  only represents the effective voltage at the input port of the electrode for the whole modulator as a microwave component. Inside the modulator, the interaction between the microwave and the optical wave has not been taken into account. Hence, the following analyses come out.

## 2.2 Phase velocity mismatch between the microwave and the optical wave

The EOIM is no doubt also an optical component. Once the microwave is injected into the modulator, the optical wave transmitted through the optical waveguide can be modulated by the microwave signal through the electrodes inside the modulator. But the two waves have different frequencies, i. e., different effective refractive indices at microwave and optical frequencies, resulting in phase velocity mismatch which leads to low conversion efficiency of the electrooptic modulation. Moreover, the efficiency decreases as the frequency increases. Referring to the papers [12-13], an index,  $M$  is introduced to describe the modulation efficiency, and  $M$  is given by

$$M(f) = \left[ \frac{1 - 2e^{-\alpha L} \cos \theta + e^{-2\alpha L}}{(\alpha L)^2 + \theta^2} \right]^{1/2}, \quad (7)$$

where  $\theta = \frac{\omega_m L(n_m - n_o)}{c}$ ;  $\omega_m$  is the modulated angular frequency;  $\alpha$  is the conductor loss;  $L$  is the interaction length of the electrode;  $c$  is the velocity of light in vacuum;  $n_m$  and  $n_o$  are effective refractive indices of the microwave and the optical wave in the modulator, respectively.

Then, considering Eq. (6) and (7), the modulation depth  $C$  is expressed as

$$C = C_0 M. \quad (8)$$

When the modulator is packaged, the structure parameters of the component, like the length of the electrode  $L$ , the effective refractive indices  $n_m - n_o$  (with respect to the input light, the bandwidth, and the driving voltage of the modulator at design), etc., are given. The modulation depth only depends on the outside modulated signal. Hence,  $C$  can be written as  $C = C(P_m, f_m)$ , which means by tuning the microwave power at a fixed frequency, the appropriate  $C$  can be chosen to obtain the optimal modulated sideband at a proper DC bias for some specific application.

## 3 Experiment

Experiments have been carried out to verify Eq. (8). Fig.3 indicates the experimental block diagram. The optical spectrum analyzer (ADVANTEST Q8384) (OSA) is

used to measure the output optical spectrum of the EOIM. The actual modulation depth is obtained by the ratio of the intensities of the even or the odd sidebands as Eq. (4) described. Fig.4 shows the experimental  $C$  values as stars and the theoretical results calculated from Eq. (8) as rings. Parameters are chosen according to the 15 Gbit/s EOIM we used, given as  $L = 35$  mm,  $\alpha = 0.5$  dB/ $\sqrt{\text{GHz}} \cdot \text{cm}$ ,  $n_m - n_o = 0.18 \sim 0.22$ . Besides the inexact measured values (limited by the highest wavelength resolution of the OSA 0.01 nm) at low frequency ( $\leq 3$  GHz), good agreement between theoretical analyses and experimental results is presented. However, the modulation depth is limited by the maximum microwave power applied to the modulator (27 dBm for the EOIM we used). To take the distributed Brillouin optical fiber sensing for example,  $C \approx 0.9$  (at  $P_m = 26$  dBm and  $f_m = 11$  GHz) as Fig. 4 shows, means that the intensity of the first sideband with Brillouin frequency shift is much smaller than its theoretical maximum value (where  $C \approx 1.8$  makes  $J_1(C)$  maximum). Hence, an EOIM need to be tested first to judge whether it can provide sufficient modulation for some application or not. On the other hand, based on characteristics of the EOIM itself, appropriate microwave power and frequency can be chosen to obtain the appropriate modulation depth following the estimation that we present here. The appropriate modulation depth then optimizes the desired sideband of the system through a proper transimission bias.

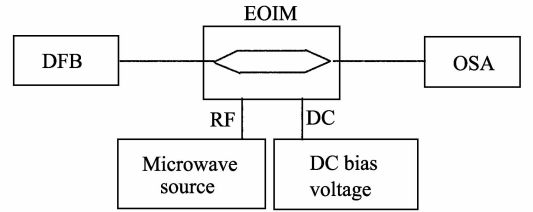


Fig. 3 Experimental block diagram of the modulation depth measurement

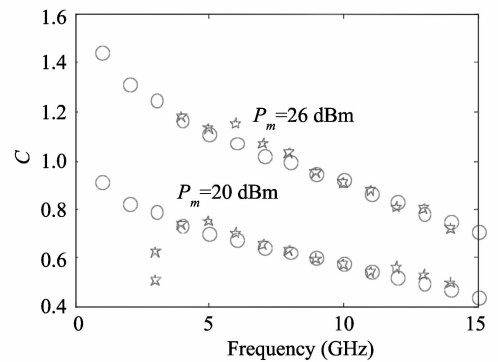


Fig. 4 The theoretical and experimental modulation depth Conclusion

The modulation depth has been put forward to estimate the frequency-shift performance of the EOIM. In theory, the modulation depth has been analyzed from two

aspects, impedance mismatch and phase velocity mismatch. The effective voltage applied to the RF port of the modulator has been calculated from the microwave power and frequency. The experimental results agree well with the theoretical analyses. The appropriate modulation depth can be achieved by tuning the microwave power and frequency for a desired modulated sideband. Results obtained here is not only useful for the Brillouin optical fiber sensing, but also for optical communication and microwave photonics based on the frequency shift characteristic of the EOIM.

## References

- [1] M. Song, B. Zhao, X. Zhang, 2005. Optical coherent detection Brillouin distributed optical fiber sensor based on orthogonal polarization diversity reception. *Chin. Opt. Lett.*, 3: 271.
- [2] S. Foaleng-Mafang, J. C. Beugnot, L. Thévenaz, 2009. Optimized Configuration for High Resolution Distributed Sensing Using Brillouin Echoes. *Proc. SPIE 7503*, 75032C.
- [3] A. Zornoza, D. Olier, M. Sagues, et al, 2009. Distortion-free Brillouin Distributed Sensor Using RF Shaping of Pump Pulses. *Proc. SPIE 7503*, 75036D.
- [4] J. Kondo, K. Aoki, Y. Iwata, et al, 2005. 76-GHz Millimeter-wave Generation Using MZ LiNbO<sub>3</sub> Modulator with Drive Voltage of 7 Vp-p and 19 GHz Signal Input. *Microwave Photonics*.
- [5] A. Loayssa, C. Lim, A. Nirmalathas, et al, 2003. Design and performance of the bidirectional optical single-sideband modulator. *J. Lightwave Technol.*, 21: 1071.
- [6] D. Xiang, L. Liu, G. Chen, et al, 2006. Optical waveguide phase modulation technology for generating multi-wavelength optical source. *Opto-Electronic Engineering*, 33: 73.
- [7] M. Niklès, L. Thévenaz, P. A. Robert, 1996. Simple distributed fiber sensor based on Brillouin gain spectrum analysis. *Opt. Lett.*, 21: 758.
- [8] H. Zhou, Z. Meng, Y. Liao, 2009. Study of frequency shift characteristics based on LiNbO<sub>3</sub> waveguide electro-optic intensity modulator. *Chin. J. Lasers*, 36: 901.
- [9] Z. Meng, H. Zhou, Y. Liao, et al, 2008. Measurement of Frequency Shift Characteristic Based on LiNbO<sub>3</sub> Waveguide Electro-optic Intensity Modulator. *Proceeding of 2008 1st Asia-Pacific Optical Fiber Sensors Conference*.
- [10] Y. Liao, H. Zhou, Z. Meng, 2009. Modulation efficiency of a LiNbO<sub>3</sub> waveguide electro-optic intensity modulator operating at high microwave frequency. *Opt. Lett.*, 34: 1822.
- [11] K. Yoshida, Y. Kanda, S. Kohjiro, 1999. A traveling-wave-type LiNbO<sub>3</sub> optical modulator with superconducting electrodes. *IEEE Transactions on Microwave Theory and Techniques*, 47: 1201.
- [12] K. Yoshida, A. Minami, 1997. Traveling-wave type LiNbO<sub>3</sub> optical modulator with a superconducting coplanar waveguide electrode. *IEEE Transactions on Applied Superconductivity*, 7: 3508.
- [13] A. Ahmed, Abou El-Fadl, A. I. Zarea, 2006. Modeling and Analysis of LiNbO<sub>3</sub> Optical Modulator with Superconducting Electrodes. *IEEE CCECE/CCGEI*.
- [14] G. K. Gopalakrishnan, W. K. Burns, R. W. McElhanon, et al, 1994. Performance and modeling of broadband LiNbO<sub>3</sub> traveling wave optical intensity modulators. *J. Lightwave Technol.*, 12(10): 1807.
- [15] K. Noguchi, O. Mitomi, H. Miyazawa, 1998. Millimeter-wave Ti:LiNbO<sub>3</sub> optical modulators. *J. Lightwave Technol.*, 16(4): 615.